NASA TECHNICAL NOTE

NASA TN D-3453

NASA TN D-3453

MATHEMATICAL MODEL WITH EXPERIMENTAL VERIFICATION FOR THE DYNAMIC BEHAVIOR OF A SINGLE-TUBE CONDENSER

by Andrew A. Schoenberg

Lewis Research Center
Cleveland, Ohio

NATIONAL AERONAUTICS AND SPACE ADMINISTRATION • WASHINGTON, D. C. • JUNE 1966

MATHEMATICAL MODEL WITH EXPERIMENTAL VERIFICATION FOR THE DYNAMIC BEHAVIOR OF A SINGLE-TUBE CONDENSER

By Andrew A. Schoenberg

Lewis Research Center
Cleveland, Ohio

NATIONAL AERONAUTICS AND SPACE ADMINISTRATION

For sale by the Clearinghouse for Federal Scientific and Technical Information
Springfield, Virginia 22151 – Price $3.00

MATHEMATICAL MODEL WITH EXPERIMENTAL VERIFICATION FOR THE DYNAMIC BEHAVIOR OF A SINGLE-TUBE CONDENSER

by Andrew A. Schoenberg

Lewis Research Center

SUMMARY

A mathematical model is derived to predict the dynamic behavior of a single-tube condenser. The tube is assumed to contain a mobile liquid-vapor interface and to be cooled by a gas or liquid stream in crossflow. The model consists of transfer functions relating the condensing pressure and the interface position to various disturbance variables. The transfer functions are derived from the linearized form of the fundamental heat-transfer and flow equations of the process.

The part of the model relating the condensing pressure and the interface movement to vapor flow variations is verified by comparison of predicted with experimental frequency responses of a gas-cooled mercury condenser. Good agreement is found for the amplitude and the phase of the condensing pressure response and the amplitude response of the interface movement. The phase lag of the interface movement, however, is considerably greater than predicted. This disagreement is attributed to the liquid droplet transport delay time which was neglected in the theory.

The two verified transfer functions are in the form of third- over fourth-order polynomials. The break frequencies of the transfer functions depend on the steady-state operating point. This condition is illustrated by changes in the experimental frequency response of the pressure and interface when the operating point is changed. The same change is predicted by the model, thus giving further evidence of its validity.

An additional investigation is made of the variations of the model due to uncertainty in evaluating some of the transfer function parameters. The predicted frequency responses are found to be sensitive to several of the process properties, such as the heat-transfer coefficients and the vapor and liquid pressure drop functions.

Some of the values of the coefficients of the transfer functions for the cases investigated are very small and, hence, have little influence on the predicted frequency responses. When these values are neglected, a much simpler form of the transfer functions is arrived at, which agrees well at the lower frequencies with the original more complex model.

INTRODUCTION

The condensation of the working fluid in Rankine power cycles has gained increased attention due to the development work on space electric power generators such as SNAP-8. In these high performance systems where reliability and unattended operation are essential, the excursions of the condensing process from the design conditions due to various disturbances must be kept within narrow limits. Changes of the condensing pressure are of special importance because high turbine back pressure reduces efficiency, while low pressure may cause pump cavitation and eventual system deterioration. To predict these pressure variations and to control them, the dynamic or transient behavior of the condensing process must be understood.

Previous work in heat exchanger dynamics (refs. 1 and 2) has treated the response of liquid coolant temperature due to variations in condensing pressure. However, no analytic or experimental studies were found where condensing pressure is assumed to be the dependent variable, that is, where the disturbances in the system originate in the vapor flow or coolant variations. An additional constraint, which has not been considered by previous investigators, is the existence of a mobile liquid-vapor interface. In the type of system of interest here, the position of the interface in the exchanger tubes determines the heat-transfer area of the condensing region. This has the effect of coupling the condensing pressure to the amount of liquid inventory in the exchanger. Thus, there is a need to study the dynamics of this type of condenser, and in particular, the behavior of the condensing pressure and the vapor liquid interface.

Such studies, both experimental and analytical, were undertaken at the NASA Lewis Research Center. The experimental part of the program dealt specifically with mercury vapor condensing inside single tubes. A constant diameter steel tube cooled by gas in crossflow was used for the dynamic studies. (This choice of configuration simplified not only the instrumentation and measurements, but also eliminated the complication of coolant dynamics which must be considered in parallel or counterflow liquid cooled condenser.) In support of the experiments, as well as to develop an ability to predict time variable behavior, a theoretical model of the process was derived. The purpose of this report is to present this derivation and to show how the theory compares with experimental results.

The approach taken in deriving the theoretical model is to approximate the fundamental dynamic phenomena rather than to attempt a rigorous solution of the partial differential equations governing the condenser. The equations are simplified and linearized for small perturbations about a known steady-state operating point and then Laplace transformed to obtain the system transfer functions. This method has been used with success in the analysis of heat exchanger dynamics by various investigators (refs. 1 to 3). The derived transfer functions are then analyzed in some detail in terms of the theoretical

frequency response they predict. In this analysis an attempt is made to relate the dynamic characteristics to basic physical properties of the condensing process, such as the thermal capacitance of the tube walls, the liquid storage, and the pressure drop gradients.

In the last part of the report the predicted frequency responses for the single-tube condenser are compared with the experimentally obtained responses to establish the accuracy of the theory. The experimental results used in the comparison are part of the data obtained for the mercury condensing dynamics program.

Two questions arising in the determination of the theoretical frequency response are examined in separate sections of the report. One section deals with the error in prediction of frequency response due to uncertainty of some of the process properties. The other is concerned with the possible simplification of the transfer functions.

Although the derivation and discussions are applied specifically to a mercury condensing tube, the theory is general enough to be applicable to other condensers which are uniformly cooled and contain a vapor-liquid interface. For added generality, the derivation of the basic condenser element is carried out separately from the inlet and outlet pressure-to-flow characteristic of the condenser. This permits simple modification of the model so as to include other condenser inlet and outlet conditions.

THEORY DERIVATION

Herein is presented the derivation of the mathematical model used to predict the variations of the condensing pressure and interface due to various disturbances in the process. The disturbance variables are assumed to be the vapor input flow rate, the receiver pressure, and the coolant temperature.

The analysis itself is divided into three sections. The first deals with the derivation of the transfer functions for the condensing pressure variations, assuming the interface movement to be an independent variable. In the second section, the transfer functions for the interface are derived, assuming in turn that the condensing pressure is an input variable. In the last part of the derivation, the two transfer functions are analyzed and then combined to obtain the desired model for the pressure and interface behavior of the total condensing process.

Condenser Description

The condenser that is analyzed is shown schematically in figure 1. It consists of a

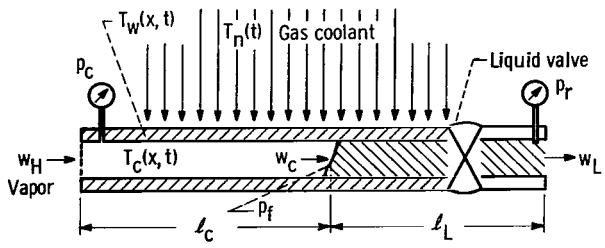

Figure 1. - Schematic of condensing tube.

single tube with inside and outside diameters D_1 and D_2, respectively. The tube wall temperature $T_w(x, t)$ is a function of both the axial position from the inlet x and time t. The tube is convectively cooled by a cross-flow gas stream at a temperature $T_n(t)$. The inlet vapor flow rate w_H is determined by a choked valve so that this flow rate into the tube can be assumed independent of any changes in the downstream conditions.

The total condensing flow rate w_c depends on the heat flow into the wall of the tube. This heat flow is proportional to the difference between the condensing temperature $T_c(x, t)$ and the wall temperature $T_w(x, t)$ multiplied by the coefficient of heat transfer. The vapor has to condense completely over the condensing length ℓ_c, which is determined by the location of the liquid-vapor interface. The remaining length of the tube ℓ_L is filled with liquid that is subcooled and then exhausted into the receiver.

The liquid outflow rate w_L is determined by the liquid flow characteristics of the valve at the exit of the tube and the difference in pressures at the interface p_f and the receiver p_r.

Derivation of Condensing Pressure Transfer Function with Interface Position as Independent Variable

The equations that govern the heat transfer and fluid flow of the condenser just described are

$$(1 - X_q)w_H(t) + w_c(t) - w_L(t) = -\rho_L \frac{dV_v}{dt} \tag{1}$$

$$X_q w_H(t) - w_c(t) = \frac{d}{dt}(\rho_v V_v) \tag{2}$$

$$H_L w_c(t) = \int_0^{\ell_c(t)} h_{cw}\pi D_1\left[T_c(x, t) - T_w(x, t)\right]dx \tag{3}$$

$$\frac{dT_w(x, t)}{dt} = \frac{4D_1 h_{cw}}{\rho_w c_w\left(D_2^2 - D_1^2\right)}\left[T_c(x, t) - T_w(x, t)\right] - \frac{4D_2 h_{nw}}{\rho_w c_w\left(D_2^2 - D_1^2\right)}\left[T_w(x, t) - T_n(t)\right] \tag{4}$$

(All symbols are defined in appendix A.) Equation (1) expresses the continuity relation for the liquid phase. It states that the sum of the condensing flow w_c and the liquid input flow rate $(1 - X_q)w_H$ minus the liquid outflow w_L must equal the net rate of decrease of the product of gas phase volume and the liquid density ρ_L. The quality of the input stream is X_q. The second equation similarly states the conservation of mass in the gas phase. The density of the gas ρ_v is for simplicity taken to be that at the tube inlet.

The third equation represents the heat-transfer process in the vapor region of the condenser. The right-hand side is the heat flux into the wall. The left-hand side is the heat flux given up by the vapor during condensation. The assumptions made here are that (1) the amount of internal energy change in the gas phase is negligible and (2) the heat content of the input stream is the heat of vaporization H_L with a negligible amount of superheat energy.

The fourth equation states the heat flux balance from the condensing region to the coolant. It includes a heat storage term due to the wall heat capacity. The wall is considered as having a uniform temperature in the radial direction.

Two additional assumptions are made to allow the integration of equation (3). The coefficient of heat transfer between condensate and wall h_{cw} is assumed constant. Its variation will generally not affect the heat transfer significantly since its value is much larger than that of the coolant side. This is particularly true for the gas-cooled tube used in this investigation.

The other assumption is that the condensing temperature variation along the length x can be approximated in the steady state by

$$T_c(x, t) = T_c(t)(1 - mx) \tag{5}$$

This form is introduced to account for a significant pressure drop in the vapor region noted for some operating conditions of the condenser tube. An example of the temperature profile is given in figure 19 in appendix B. The effect of equation (5) is to introduce the average of inlet and outlet condensing temperature for the steady-state heat-transfer calculations. Variations in m are neglected so that dynamically the average temperature is assumed to vary as the inlet temperature.

To relate the gas phase density and the condensing temperature to the condensing pressure, the perfect gas law and the Clausius-Clapeyron equation, respectively, are used:

$$\rho_v = \frac{p_c}{RT_c} \tag{6}$$

and where R = gas constant

$$\frac{dp_c}{dT_c} = \frac{H_L p_c}{RT_c^2} \tag{7}$$

Another relation needed for the simultaneous solution of the first four equations is

$$V_v(t) = A_c \ell_c(t) \tag{8}$$

where $V_v(t)$ is the volume of the gas phase, A_c the cross-sectional area of the tube, and $\ell_c(t)$ the condensing length.

Several assumptions are implied in this formulation of the vapor volume. First, it is assumed that the liquid droplets inside the vapor take up an insignificant amount of volume. This is justified due to the large density difference between the gas and liquid phases (3000:1 for mercury at 16 psia). Also assumed is a distinct liquid-vapor interface that moves inside the tube in a piston-like manner when the liquid inventory of the condenser changes. A less obvious implication of equation (8) together with equation (1) is that the liquid condensate collects at the interface without significant time delay. This assumption, although not quite accurate, avoids the great complexity of formulating a valid model of droplet formation and velocity.

Conceptually these eight equations plus specified initial conditions are sufficient to determine the condensing pressure in terms of the input flow w_H, the condensing length, and the coolant gas temperature. The nonlinearity of some of the equations and the complex interdependencies of the variables, however, make it more practical to solve them in a simpler linearized form.

The simplification consists of linearizing the equations by considering only small perturbations of the variables about a known steady-state operating point. The linearized differential equations can then be Laplace transformed and solved algebraically to obtain the transfer functions relating the condensing pressure to the disturbance variables.

The linearization does limit the predictive ability of the model, particularly when large changes in the operating point are considered. Where the disturbances are reasonably small, however, such as expected during normal operation of the Rankine loop or for sinusoidal testing, the simplifications will not detract significantly from the accuracy of the predicted dynamic response.

The variation of the variables about their steady-state values can be written as

$$w_H(t) = \overline{w_H} + \Delta w_H(t)$$

$$\ell_c(t) = \overline{\ell_c} + \Delta \ell_c(t)$$

and similarly for all other variables. Substituting these into equations (1) to (8), eliminating the steady-state parts, and Laplace transforming with respect to the time variable result in the following equations (s is the Laplace operator):

$$(1 - X_q)\Delta w_H(s) + \Delta w_c(s) - \Delta w_L(s) = -\rho_L s\, \Delta V_v(s) \tag{1a}$$

$$X_q\, \Delta w_H(s) - \Delta w_c(s) = \bar{\rho}_v s\, \Delta V_v(s) + \bar{V}_v s\, \Delta \rho_v(s) \tag{2a}$$

$$H_L\, \Delta w_c(s) = \int_0^{\bar{\ell}_c} h_{cw}\pi D_1\left[\Delta T_c(x, s) - \Delta T_w(x, s)\right]dx + h_{cw}\pi D_1\left[\bar{T}_c(\bar{\ell}_c, 0) - \bar{T}_w(\ell_c, 0)\right]\Delta \ell_c(s) \tag{3a}$$

$$\Delta T_w(x, s)(\tau_w s + 1) = K_{1w}\, \Delta T_c(x, s) + K_{2w}\, \Delta T_n(s) \tag{4a}$$

where

$$\tau_w \equiv \frac{\rho_w c_w \left(D_2^2 - D_1^2\right)}{4(h_{cw}D_1 + h_{nw}D_2)}$$

$$K_{1w} \equiv \frac{h_{cw}D_1}{h_{cw}D_1 + h_{nw}D_2}$$

$$K_{2w} \equiv \frac{h_{nw}D_2}{h_{cw}D_1 + h_{nw}D_2}$$

$$\Delta T_c(x, s) = \Delta T_c(s)(1 - mx) \tag{5a}$$

$$\Delta \rho_v(s) = \frac{\Delta p_c(s)}{R\bar{T}_c} - \frac{\Delta T_c(s)\bar{p}_c}{R\bar{T}_c^2} \tag{6a}$$

$$\Delta p_c(s) = \left.\frac{dp_c}{dT_c}\right|_{\bar{p}_c} \Delta T_c(s) \tag{7a}$$

$$\Delta V_v(s) = A_c\, \Delta \ell_c(s) \tag{8a}$$

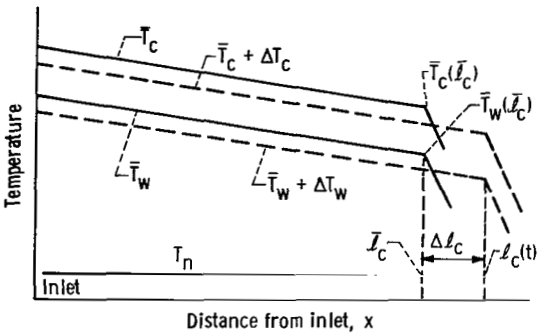

Figure 2. - Idealized temperature profile for condensing region showing expected variations.

The second term on the right-hand side of equation (3a) represents the variation of heat flux due to changes in condensing length. It is the product of the integrand evaluated at the interface position ℓ_c and the increment of interface $\Delta\ell_c(t)$.

The variations represented by equations (3a) and (7a) are shown schematically in figure 2. Note the change in overall level of condensing temperature $\Delta T_c(t)$ at a constant slope of the profile and the change in condensing length, which is accounted for by the change in the limit of integration. The terms of the other equations are obtained directly by proper substitutions of the variations.

The integral of equation (3a) can be evaluated by assuming a constant h_{cw} and by employing the relations of equations (4a) and (5a). In dimensionless form, equation (3a) becomes

$$W_c = Z_L \frac{(\tau_{1w}s + 1)}{(\tau_w s + 1)} \frac{\Delta T_c(s)}{T_a} - \frac{C_n}{\tau_w s + 1} + L_c \tag{9}$$

where

$$W_c \equiv \frac{\Delta w_c(s)}{\bar{w}_c}$$

$$Z_L \equiv 1 - \frac{m\bar{\ell}_c}{2}$$

$$T_a \equiv \bar{T}_c Z_L - \bar{T}_n$$

$$\tau_{1w} \equiv \frac{\rho_w c_w \left(D_2^2 - D_1^2\right)}{4h_{nw} D_2}$$

$$C_n \equiv \frac{\Delta T_n(s)}{T_a}$$

$$L_c \equiv \frac{\Delta \ell_c(s)}{\bar{\ell}_c}$$

and where the following steady-state equalities have been used:

$$\bar{w}_c H_L = \frac{h_{cw} \pi D_1 h_{nw} D_2 \bar{\ell}_c T_a}{h_{cw} D_1 + h_{nw} D_2}$$

$$\bar{w}_c H_L = h_{cw} \pi D_1 \bar{\ell}_c \left[T_c\left(\bar{\ell}_c\right) - T_w\left(\bar{\ell}_c\right) \right]$$

Equation (9) represents the overall dynamic heat balance of the condensing region, which is the basis of the condenser model developed in this report.

The condensing flow W_c and the condensing temperature variation $\Delta T_c/T_a$ can be written in terms of the input flow, the condensing length, and the pressure by employing equations (2a), (6a), (7a), and (8a). The desired relations for condensing flow is

$$W_c = W_H - \theta s L_c - (1 - \beta_x)\theta s P_c \tag{10}$$

where

$$W_H \equiv \frac{\Delta w_H(s)}{\bar{w}_H}$$

$$\theta \equiv \frac{\bar{\rho}_v A_c \bar{\ell}_c}{X_q \bar{w}_H}$$

$$\beta_x = \frac{\bar{p}_c}{\bar{\rho}_v H_L J}$$

in which for steady state

$$\bar{w}_H = \frac{w_c}{X_q} = \bar{w}_L$$

The relation for the condensing temperature variation is

$$\frac{\Delta T_c}{T_a} = \left(\frac{\bar{p}_c}{T_a \left. \frac{dp_c}{dT_c} \right|_{\bar{p}_c}} \right) P_c \tag{11}$$

where again

$$P_c = \frac{\Delta p_c(s)}{\bar{p}_c}$$

Substituting these equations into equation (9), combining like terms, and solving for P_c yield

$$P_c = \frac{G_s}{K_t} \left[W_H + \frac{C_n}{\tau_w s + 1} - (1 + \theta s) L_c \right] \tag{12}$$

where

$$G_s(s) = \frac{1 + \tau_w s}{a_s s^2 + b_s s + 1} \tag{13}$$

$$a_s \equiv \frac{\tau_w (1 - \beta_x)\theta}{K_t}$$

$$b_s \equiv \tau_{1w} + \frac{(1 - \beta_x)\theta}{K_t}$$

and

$$K_t \equiv \frac{Z_L \bar{p}_c}{\bar{T}_a} \frac{dT_c}{dp_c}$$

Equation (12) represents the desired dynamic model, which relates the condensing pressure variations to the inlet vapor flow, the coolant temperature, and the interface varia-

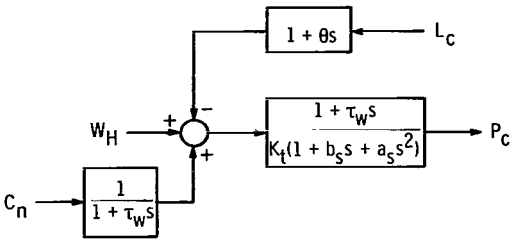

Figure 3. - Block diagram for condensing pressure variation with condensing length L_c as independent input.

tions. Figure 3 shows in block diagram form the relations involved.

The model is expressed in the form of transfer functions which may be used directly to obtain the frequency response characteristic for sinusoidal input variables or may be transformed back to the time domain for arbitrary disturbance functions of time. The variables are expressed in dimensionless form to emphasize the basic dynamic elements and the essential parameters of the model. The model is sufficient to predict dynamic behavior where the input variables, particularly the interface movement, are specified independently. In the case of the condenser tube used for the dynamic tests or condensers of similar geometries, however, where the interface movement is not independent of the other process variables, the dynamic model is not complete. The interactions between the condensing pressure and the interface movement must be established. This is done in the next section.

Derivation of Interface Transfer Function

The interface movement is strongly dependent on the exit condition and the pressure drop characteristics of the condenser. The derivation of the mathematical model describing this movement is carried out for the case where the condensate exhausts into a receiver, whose pressure is independent of the process. This is not the most general exit condition; however, the equations can easily be adapted to fit other cases such as a pump.

The receiver has the special characteristic of controlling the pressure at the interface. This is a result of the small pressure drop that exists in the liquid column between the interface and the receiver. The pressure is controlled by the movement of interface due to the imbalance between liquid outflow and condensing flow, which occurs in the direction so as to restore the pressure equilibrium on the liquid column.

The equations relating the interface movement to the various flows are already formulated in the previous section and are expressed in linearized form by equations (1a) and (2a). Adding the two equations eliminates the unknown condensing flow and results in the expression for interface movement as given in equation (14), where the variables are again expressed in dimensionless form:

$$L_c = \frac{W_L - W_H}{X_q \theta s\left(\frac{\rho_L}{\bar{\rho}_v} - 1\right)} + \frac{(1 - \beta_x)P_c}{\frac{\rho_L}{\bar{\rho}_v} - 1} \tag{14}$$

Equation (14) can be simplified by noting that the term $(1 - \beta_x)P_c/\left[(\rho_L/\bar{\rho}_v) - 1\right]$, which accounts for the change in mass in the gas phase due to changes in pressure, is very small in comparison to mass changes due to liquid changes in the interface. With the pressure term eliminated, equation (14) takes the form

$$L_c = \frac{W_L - W_H}{sX_q \theta\left(\frac{\rho_L}{\bar{\rho}_v} - 1\right)} \tag{15}$$

The next step in the derivation is to determine the liquid outflow W_L in terms of the known process variables. The approach to the problem is to consider the behavior of a liquid column moving inside a tube with frictional pressure drop. The driving force for this movement is the fluctuation of the pressure difference between the interface and the receiver. These pressures are coupled to the condensing inlet pressure through the two-phase and the liquid pressure drop characteristic of the condenser tube.

The fluid force balance for the liquid column inside the tube is

$$(p_f - p_r)A_c = A_c q_L(w_L) + M_L \frac{dv_L}{dt} \tag{16}$$

where $(p_f - p_r)$ is the pressure difference between the interface and the receiver, $q_L(w_L)$ represents the frictional pressure drop in the liquid region which is assumed a function of flow rate only, and M_L is the inertial mass of the liquid column being accelerated relative to the tube at the rate dv_L/dt. Also the following equalities should be noted:

$$M_L = \rho_L A_c \bar{\ell}_L \tag{17}$$

$$v_L = \frac{w_L}{\rho_L A_c} \tag{18}$$

The pressure at the interface, as given by equation (19), differs from the condensing inlet pressure by the pressure drop in the vapor region q_v. This pressure drop depends

primarily on the two-phase friction factor, the velocity, and the length of the vapor region. Thus, in general, q_v is assumed to vary with flow rate and condensing length:

$$p_f = p_c - q_v(w_H, \ell_c) \tag{19}$$

Substituting equations (17), (18), and (19) into equation (16) and linearizing yield

$$\Delta p_c - \frac{\partial q_v}{\partial w_H}\Delta w_H - \frac{\partial q_v}{\partial \ell_c}\Delta \ell_c - \Delta p_r = \frac{\partial q_L}{\partial w_L}\Delta w_L + \frac{\overline{\ell}_L}{A_c}\frac{d(\Delta w_L)}{dt} \tag{20}$$

where $\partial q_v/\partial w_H$, $\partial q_v/\partial L_c$, and $\partial q_L/\partial w_L$ are partials of the pressure drop which must be evaluated from steady-state experimental or theoretical relations.

It should be noted that to be strictly correct, the slope m of the temperature profile of equation (5) should be coupled to the pressure drop. For simplicity, however, the effect of the pressure drop variations on m is neglected.

Laplace transforming and changing to dimensionless form allow equation (20) to be solved for W_L:

$$W_L = \frac{K_p(P_c - P_r) - K_w W_H - K_v L_c}{\tau_p s + 1} \tag{21}$$

where

$$K_p \equiv \frac{\overline{p}_c}{w_H\left(\frac{\partial q_L}{\partial w_L}\right)}$$

$$P_r \equiv \frac{\Delta p_r}{\overline{p}_c}$$

$$K_w \equiv \frac{\left(\frac{\partial q_v}{\partial w_H}\right)}{\left(\frac{\partial q_L}{\partial w_L}\right)}$$

$$K_v \equiv \frac{L_c \dfrac{\partial q_v}{\partial \ell_c}}{w_H \dfrac{\partial q_L}{\partial w_L}}$$

$$\tau_p = \frac{\bar{\ell}_L}{A_c \dfrac{\partial q_L}{\partial w_L}} \tag{22a}$$

The conversion factor g must be included in equation (21a) for English units where q_L is in psi; therefore,

$$\tau_p \equiv \frac{\ell_L}{A_c \dfrac{\partial q_L}{\partial w_L} g} \tag{22b}$$

Equation (21) is now combined with equation (15) to eliminate W_L:

$$L_c = \frac{1}{\theta_r s}\left[\frac{K_p(P_c - P_r) - K_w W_H - K_v L_c}{1 + \tau_p s} - W_H\right] \tag{23}$$

where

$$\theta_r \equiv X_q \theta\left(\frac{\rho_L}{\rho_v} - 1\right)$$

Solving for L_c and combining similar terms give the desired transfer functions relating the interface movement to the other condenser variables:

$$L_c = G_i(s)(P_c - P_r) - \left(\frac{1 + K_w}{K_p}\right)(1 + \tau_{1p} s)G_i(s)W_H \tag{24}$$

where

$$G_i(s) \equiv \frac{K_p}{K_v(as^2 + bs + 1)} \tag{25}$$

$$a \equiv \frac{\theta_r \tau_p}{K_v}$$

$$b = \frac{\theta_r}{K_v}$$

$$\tau_{1p} \equiv \frac{\tau_p}{1 + K_w}$$

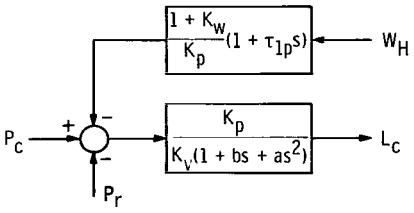

Figure 4. - Block diagram for dynamic model of interface movement.

Equation (24) is shown in block diagram form in figure 4.

This completes the derivation of the mathematical model for the dynamic behavior of the interface for the case where the condensate exhausts into a pressurized receiver. In the next section this behavior and how it interacts with the condensing pressure will be examined.

Analysis and Synthesis of Transfer Functions

In this section a closer look will be taken at the two parts of the dynamic model derived in the previous sections in order to arrive at a better understanding of the elements that determine the time-variable behavior of the condensing process. This is done by analyzing the frequency response characteristics and the coefficients of the major transfer functions. In the last part of this section the derivation of the model of the condenser as a whole interacting process is completed. This is done by the synthesis of the two previously derived elements.

The major dynamic element of the model shown in figure 3 is the transfer function defined by equation (13), $G_s(s)$. It relates the condensing pressure to the input flow variations when the other input variables of equation (12), C_n and L_c, are assumed zero. This transfer function in factored form is

$$\frac{P_c}{W_H} K_t = \frac{1 + \tau_w s}{(\tau_1 s + 1)(\tau_2 s + 1)} \tag{26}$$

where

$$\tau_1 = \frac{2a_s}{b_s\left(1 + \sqrt{1 - \frac{4a_s}{b_s^2}}\right)} \tag{27}$$

$$\tau_2 = \frac{2a_s}{b_s\left(1 - \sqrt{1 - \frac{4a_s}{b_s^2}}\right)} \tag{28}$$

This factoring is convenient when the parameter inside the square root $\left(4a_s/b_s^2\right)$ is less than 1. This also means that the denominator has two positive real roots or, in control terms, the system is overdamped.

Examination of the constants shows that this overdamped situation prevails as long as the time constants of the wall τ_{1w} and τ_w are considerably larger than the vapor capacity time constant θ. These time constants have the following physical significance. The constant τ_{1w} is the time, in seconds, required to raise the average wall temperature by 1^o when the heat flow into the wall is induced by a constant 1^o temperature difference between the wall and the coolant. The definition of τ_w differs from that of τ_{1w} only in that the heat flux into the wall is induced by a unit temperature difference between the wall and both the coolant and the condensate side. Thus, τ_{1w} is always greater than τ_w. The time constant θ (see eq. (10)) is the time in seconds for the mass in the gas phase $\bar{\rho}_v \bar{V}_v$ to be replaced at the steady-state vapor input flow rate $X_q \bar{w}_H$.

For the case where the parameter $4a_s/b_s^2$ is small, say less than 0.1, a conceptually simplified transfer function may be obtained by expanding the square root term in a Taylor series where only the first term is significant:

$$\sqrt{1 - \frac{4a_s}{b_s^2}} \cong 1 - \frac{2a_s}{b_s^2}$$

Substituting this approximation into equations (27) and (28) results in a simplified form of τ_1 and τ_2:

$$\tau_1 \cong \tau_{1a} = \frac{a_s}{b_s - \frac{a_s}{b_s}} \cong \frac{a_s}{b_s} \tag{29}$$

and

$$\tau_2 \cong \tau_{2a} = b_s \cong \tau_{1w} \tag{30}$$

The approximate frequency response is obtained by substituting the values of τ_{1a} and τ_{2a} and the sinusoidal frequency $2\pi jf$ for the operator s in equation (26) (note that f is in units of cps):

$$G_s(2\pi jf) = \frac{1 + 2\pi jf\tau_w}{(1 + 2\pi jf\tau_{1a})(1 + 2\pi jf\tau_{2a})} \tag{31}$$

Since the general inequality relation

$$\tau_{2a} > \tau_w > \tau_{1a}$$

is known, the shape of the amplitude and phase characteristic can be predicted as shown in figures 5(a) and (b).

At the lower frequency range, where $f < 1/(2\pi\tau_{1a})$, the condensing pressure response to input flow rate diminishes with increasing frequency in the form of a lag-lead with corner frequencies at $1/(2\pi\tau_{2a})$ and $1/(2\pi\tau_w)$. At higher frequencies, above $1/(2\pi\tau_{1a})$, the fluctuations of the flow rate are absorbed by the gas phase mass capacity so that the condensing pressure variations continue to diminish as frequency increases.

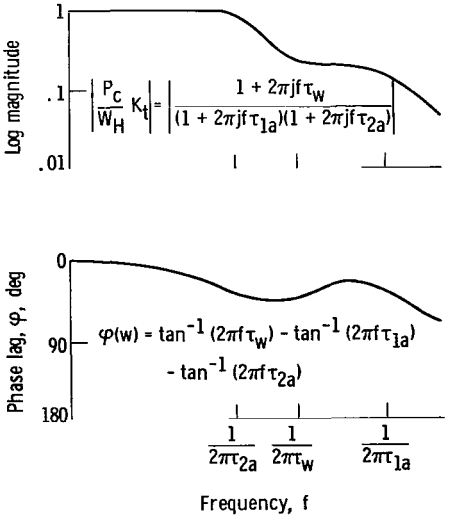

Figure 5. - Shape of frequency response of condensing pressure to vapor flow assuming no interface movement ($L_c = 0$).

It should be emphasized that this discussion applies to the condenser with a constant interface ($L_c = 0$). When this is not the case, such as with a receiver attached to the exit of the tube, the condensing pressure response to flow rate variation may change significantly.

To understand how the interface may behave, the second of the two derived models, as shown by the block diagram of figure 4, will be analyzed. When it is assumed that all the input disturbances in equation (24) except the condensing pressure variations are

zero, the interface movement becomes related to the condensing pressure by the transfer function of equation (25).

In general, this represents a second-order dynamic response. In this case, however, the parameters are not as simply analyzed as for the previous transfer function. No specific dynamic characteristic, that is, underdamped or overdamped, can be ascribed to this relation. Some trends in the response may be noted, however, by examining the standard natural frequency f_n and damping ratio σ of the second-order transfer function. These are expressed in terms of a and b

$$f_n \equiv \frac{1}{2\pi \sqrt{a}} \tag{32}$$

$$\sigma \equiv \frac{b}{2\sqrt{a}} \tag{33}$$

Typical values of the natural frequency and the damping ratio for the tube used in the experimantal study are $f_n = 0.422$ and $\sigma = 2.36$. Hence, the interface by itself responds as a highly overdamped second-order system.

Equations (32) and (33) can be written in more basic terms as

$$f_n = \frac{1}{2\pi} \sqrt{\frac{\partial q_v / \partial \ell_c}{\left(\bar{\rho}_L \bar{\ell}_L\right)}} \tag{32a}$$

$$\sigma \equiv \frac{1}{2} \frac{\partial q_L}{\partial w_L} A_c \sqrt{\frac{\rho_L}{\ell_L (\partial q_v / \partial L_c)}} \tag{33a}$$

From the last form several relations between the natural frequency and damping and the basic system properties become evident. The natural frequency of the interface movement increases and the damping decreases as the vapor pressure drop gradient $\partial q_v / \partial L_c$ becomes larger. A larger liquid length ℓ_L representing more inertia, decreases the natural frequency as well as the damping. The damping ratio σ increases with increasing liquid flow resistance $\partial q_L / \partial w_L$ and larger tube area A_c.

The analysis of the responses of the separate elements of the condenser model still leaves the problem of their combination and interaction. The resultant complete condenser model will now be examined.

The mathematical form for the simultaneous variation of flow rates, interface, and condensing pressure is arrived at by the combination of equations (12) and (24). Concep-

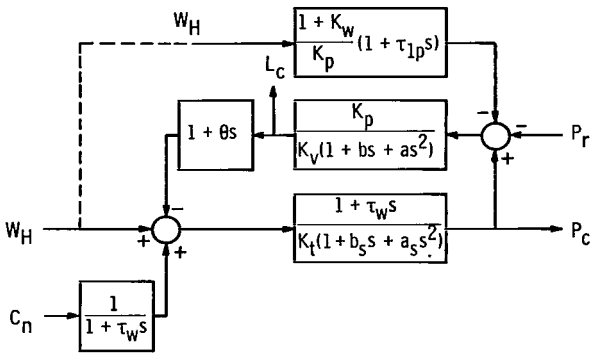

Figure 6. - Block diagram of mathematical model for dynamic behavior of condenser.

tually, this is the same as combining the block diagrams of figures 3 and 4 in the form of a multiple-loop feedback system as shown in figure 6.

The condensing pressure is solved for by substituting equation (24) for L_c in equation (12). The result is given by

$$P_c = K_{1p}G_{1p}(s)W_H + K_{2p}G_{2p}(s)C_n + K_{3p}G_{3p}(s)P_r \qquad (34)$$

with the dimensionless gain variables

$$K_{1p} = \frac{1 + \beta_v}{K_t(1 + \beta_g)} \qquad (35a)$$

$$K_{2p} = \frac{1}{K_t(1 + \beta_g)} \qquad (35b)$$

$$K_{3p} = \frac{\beta_g}{1 + \beta_g} \qquad (35c)$$

where

$$\beta_v \equiv \frac{1 + K_w}{K_v}$$

$$\beta_g = \frac{K_p}{K_v K_t}$$

The normalized transfer functions are

$$G_{1p} = G_t(1 + \tau_w s)\left(N_2 s^2 + N_1 S + 1\right) \qquad (35d)$$

$$G_{2p} = G_t(as^2 + bs + 1) \qquad (35e)$$

$$G_{3p} = G_t\left(a_L s^2 + b_L s + 1\right) \tag{35f}$$

where

$$G_t = \frac{1}{Ds^4 + Cs^3 + Bs^2 + As + 1} \tag{35g}$$

and

$$A \equiv \frac{b + b_s + b_L\beta_g}{1 + \beta_g}$$

$$B \equiv \frac{a_s + a + b_s b + \beta_g a_L}{1 + \beta_g}$$

$$C \equiv \frac{a_s b + b_s a}{1 + \beta_g}$$

$$D \equiv \frac{a_s a}{1 + \beta_g}$$

$$N_1 \equiv \frac{b + \beta_v(\tau_{1p} + \theta)}{1 + \beta_v}$$

$$N_2 = \frac{a + \beta_v \tau_{1p}\theta}{1 + \beta_v}$$

The definitions of the more basic dimensionless gains and time constants are

$$K_t = \frac{Z_L \bar{p}_c}{T_a} \frac{dT_c}{dp_c}$$

$$K_w = \frac{\left(\frac{\partial q_v}{\partial w_H}\right)}{\left(\frac{\partial q_L}{\partial w_H}\right)}$$

$$K_v = \frac{\frac{\partial q_v}{\partial L_c}\bar{\ell}_c}{\frac{\partial q_L}{\partial w_H}\bar{w}_H}$$

$$K_p = \frac{\bar{p}_c}{\bar{w}_H \frac{\partial q_L}{\partial w_L}}$$

$$a_L = \tau_w \theta \qquad \text{(sec)}$$

$$b_L = \tau_w + \theta \qquad \text{(sec)}$$

$$a = \frac{\theta_r \tau_p}{K_v} \qquad (\text{sec}^2)$$

$$b = \frac{\theta_r}{K_v} \qquad \text{(sec)}$$

$$a_s = \frac{\tau_w (1 - \beta_x)\theta}{K_t} \qquad (\text{sec}^2)$$

$$b_s = \tau_{1w} + \frac{(1 - \beta_x)\theta}{K_t} \qquad \text{(sec)}$$

$$\tau_{1w} = \frac{\rho_w c_w \left(D_2^2 - D_1^2\right)}{4 h_{nw} D_2} \qquad \text{(sec)}$$

$$\tau_w = \frac{\tau_{1w} h_{nw} D_2}{h_{nw} D_2 + h_{cw} D_1} \quad \text{(sec)}$$

$$\theta = \frac{\bar{\rho}_v \bar{V}_v}{X_q \bar{w}_H} \quad \text{(sec)}$$

$$\theta_r = X_q \theta \left(\frac{\rho_L}{\rho_v} - 1 \right) \quad \text{(sec)}$$

$$\tau_p = \frac{\ell_L}{A_c \frac{\partial q_L}{\partial w_L}} \quad \text{(sec)}$$

$$\tau_{1p} = \frac{\tau_p}{1 + K_w} \quad \text{(sec)}$$

$$\beta_x = \frac{\bar{p}_c}{\rho_v H_L J}$$

Similarly, when equation (12) is substituted into equation (24) and solved for the interface movement,

$$L_c = K_{1L} G_{1L}(s) W_H + K_{2L} G_{2L}(s) C_n - K_{3L} G_{3L}(s) P_r \tag{36}$$

The dimensionless gain constants are

$$K_{1L} = \frac{(1 - \beta_p) K_p}{K_t K_v (1 + \beta_g)} \tag{37a}$$

$$K_{2L} = \frac{K_p}{K_t K_v (1 + \beta_g)} \tag{37b}$$

$$K_{3L} = \frac{K_p}{K_v(1 + \beta_g)} \tag{37c}$$

where

$$\beta_p \equiv \frac{K_t(1 + K_w)}{K_p}$$

The normalized transfer functions are

$$G_{1L} = G_t\left(1 + M_{1L}s - M_{2L}s^2 - M_{3L}s^3\right) \tag{37d}$$

$$G_{2L} = G_t \tag{37e}$$

$$G_{3L} = G_t\left(a_s s^2 + b_s s + 1\right) \tag{37f}$$

where

$$M_{1L} = \frac{\tau_w - \beta_p(b_s + \tau_{1p})}{1 - \beta_p}$$

$$M_{2L} = \frac{\beta_p}{1 - \beta_p}(a_s + b_s\tau_{1p})$$

$$M_{3L} = \frac{a_s\tau_{1p}\beta_p}{1 - \beta_p}$$

Equations (34) and (36) represent the desired mathematical model of the condensing process. The first equation relates the percent variation of condensing pressure to percent changes of the input variables consisting of the input flow, the coolant temperature, and the receiver pressure. The second equation relates the percent variation of interface for the same input variables. The normalized forms which are shown separate the steady-state gains (the K's) from the dynamic elements (the G's). The K's define the percentage change of the output variables for percentage change in the input variables in the steady state. The G's are equal to unity for steady state, but define the transient or frequency response behavior of the condensing pressure and interface when any of the input variables change with time.

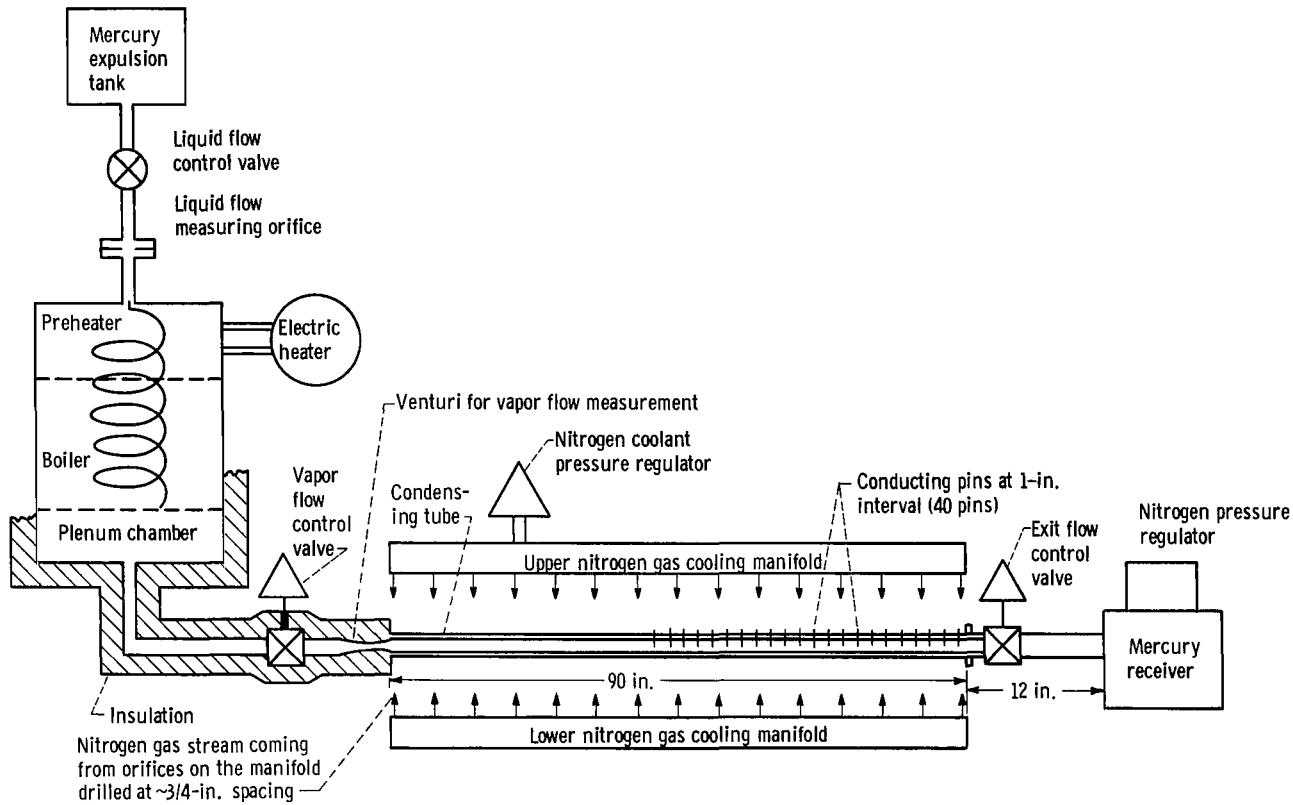

Figure 7. - Experimental rig for mercury condenser dynamic studies.

The complexity of the algebra does not allow a general discussion of the dynamic properties of the transfer functions. However, characteristic patterns in the dynamic response will be noted in the next section where the frequency responses for the experimental condenser tube are computed.

COMPARISON OF THEORY WITH EXPERIMENTAL DATA

The many simplifying assumptions and linearizations that are made in deriving the mathematical model of the condensing process raise the question of how well the model predicts the behavior of the real system. An estimate of the accuracy of the model can be obtained by comparing the analytic and the experimental frequency responses. The tube was equipped to measure the frequency response of only two of the derived transfer functions (G_{1p} and G_{1L}) so that a comparison for only these can be made. The other transfer functions are not analyzed. However, their frequency response can be easily computed by using the constants of tables II and IV (pp. 46 and 50).

The first part of this section describes how the data were obtained and how the corresponding theoretical frequency responses are calculated. The results are presented in graphical form for two different operating points. The areas of agreement and disagreement, as well as the possible sources of error, are discussed. In the last part, an attempt is made to estimate the effect of inaccuracies of various parameters on the predictability of the frequency responses.

Procedure for Obtaining Frequency Response

The test facility is shown schematically in figure 7. It consists of a horizontal stainless-steel condensing tube that is 90 inches long and has a 3/8-inch nominal outside diameter and a 1/32-inch wall. The mercury vapor, near a quality of one or slightly superheated, is generated by an electrically heated tube-type boiler. A large plenum is provided at the exit of the boiler to assure constant pressure at the inlet of the choked flow control valve during the induced flow variations. The condensing tube is cooled by nitrogen gas flowing across the tube. The gas emerges from closely spaced holes in the manifolds located above and below the tube. The condensed liquid exhausts through the exit valve into the controlled-pressure receiver.

The tube is instrumented to record the dynamic variations of condensing inlet pressure, receiver pressure, liquid pressure drop across the exit valve, interface movement, and mercury vapor flow rate. The pressures are measured by closely coupled fast response electromechanical pressure transducers. The interface movement is mea-

sured by special means based on the principle of the mercury switch. Conducting pins, electrically insulated from the tube wall, are placed at 1-inch intervals along the axis at the top of the tube. Those pins that are in contact with the liquid mercury send "on" signals which are summed to produce a voltage proportional to the length of the liquid column inside the tube. The mercury vapor flow is determined from measurements of the ΔP across a calibrated venturi at the inlet of the tube.

The experimental procedure in obtaining the frequency response data is as follows: The mercury flow rate to the condenser is set at some desired operating point by control of the inlet vapor flow control valve. The nitrogen gas coolant rate is kept constant by setting a desired manifold pressure. The liquid-vapor interface is then adjusted to the desired length by control of the receiver pressure. The steady-state gain is established by measuring the pressure and interface positions at the upper and lower limits of the flow variations to be used. These limits are set about ±10 percent of the steady-state flow $\overline{w}_H$. The instrumentation and recording equipment is checked and calibrated if necessary at this time. After this standard preliminary procedure, the frequency response tests are conducted. The vapor flow control valve is moved sinusoidally at various frequencies to introduce sinusoidal variations in mercury vapor flowing into the condensing tube. (It should be noted here that the valve is designed to provide linear variations of flow area against valve position so that in combination with the choked condition and constant upstream pressure, a sinusoidal valve movement produces corresponding vapor flow variations.) The resultant changes in the primary dependent variables - the condensing inlet pressure and the vapor liquid interface - together with the flow variations are recorded simultaneously on a direct-inking recorder. The resultant sinusoidal traces are then used to calculate the amplitudes ratio and phase shifts at each frequency. The amplitude is normalized by the amplitude obtained during steady-state calibration.

These tests are carried out for a number of operating points, that is, various levels of coolant flow rates, receiver pressure, and vapor flow rate. Only two examples, which will be called cases I and II, are presented to illustrate two distinctly different frequency responses. Case I corresponds to a long condensing length and a large pressure drop in the vapor region. Case II represents a short condensing length and a small pressure drop between inlet and receiver pressure.

Before presenting the results, however, the method of calculating the theoretical frequency response should be discussed. As mentioned previously, only the two transfer functions G_{1p} and G_{1L}, as given by equations (35d) and (37d), are considered in the comparison. The parameters entering into these transfer functions are summarized in tables II, III, and IV of appendix B. An example of the calculation of these parameters is also presented therein.

Some of the required properties of the process, in particular the pressure drop in the liquid leg of the condenser, are not accurately known. Hence, the estimated mean

values are used for the calculation. The effect of inaccuracies and changes of this and other uncertain variables on the predicted frequency response will be discussed in more detail in the Sensitivity of Predicted Frequency Response to Parameter Changes section.

Substituting the numerical values of the parameters as given in table II into equations (35d) and (37d) gives the theoretical expression for G_{1p} and G_{1L} used in the comparison with the experimental results. The results for case I are

$$\frac{P_c}{K_{1p}W_H} = G_{1p}(s) = \frac{(1 + 0.851\ s)(1 + 1.48\ s + 0.075\ s^2)}{1 + 3.86\ s + 3.40\ s^2 + 0.208\ s^3 + 0.00203\ s^4} \tag{38}$$

$$\frac{L_c}{K_{1L}W_H} = G_{1L}(s) = \frac{1 + 1.66\ s + 0.0081\ s^2 - 0.000035\ s^3}{1 + 3.86\ s + 3.40\ s^2 + 0.208\ s^3 + 0.00203\ s^4} \tag{39}$$

The form used for plotting the frequency responses is obtained by replacing s by the complex operator $2\pi jf$. The plots and their comparisons are presented next.

Results and Comparison

Figure 8(a) shows the normalized amplitude and phase of the condensing pressure response G_{1p} as a function of the frequency of the vapor flow disturbances for case I. The experimental points are shown by squares, while the theory is represented by the continuous line.

The agreement in amplitude is very good, both in the shape of the curve and the actual amplitudes over the whole frequency range. The predicted phase lag also agrees very well up to 0.1 cps, but becomes less than the data indicate in the frequency range of 0.1 to 1 cps. The phase data above 1 cps could not be measured for this case due to recording of the sinusoids with the paper speed too slow. Several factors may be responsible for this discrepancy in the 0.1 to 1 cps range. There may be some delay in the response of pressure due to the time required for establishment of thermal equilibrium between the liquid and gas phases, which has been neglected in the formulation of the Clausius-Clapeyron equation. Another delay may be introduced by the transport time required for the droplets to reach the interface. This effect will be discussed later. There is also a possibility of error in the reduction of the experimental data due to the somewhat distorted waveform of the recorded pressure oscillations.

The basic dynamic relation for case I is a lag-lead response at the lower frequencies corresponding to the time constants of the wall energy storage and the liquid inventory

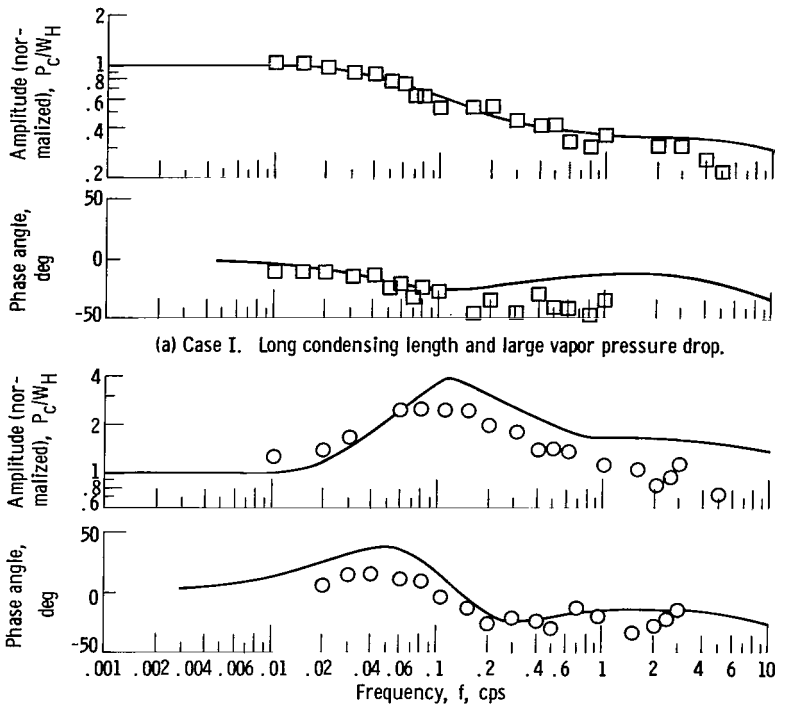

(a) Case I. Long condensing length and large vapor pressure drop.

(b) Case II. Short condensing lengths.

Figure 8. - Comparison of experimental and theoretical condensing inlet pressure frequency response to vapor flow.

capacity. At the higher frequencies above 1 cps the vapor volume capacitance begins to absorb the vapor flow oscillations, thus further diminishing the pressure response.

The condensing pressure does not necessarily respond in the same manner under all operating conditions. This condition is shown by case II. Besides the differences in condensing length noted previously, the condensing pressure and the coefficients of heat transfer for both the condensing and coolant sides are considerably higher for this case. Consequently, the parameters entering into the transfer function as shown in table II differ significantly for the two cases. Both the theoretical and experimental frequency response show a corresponding difference as can be seen in figure 8(b).

Again relatively good agreement exists between the theoretical and experimental results. At low frequency, the pressure oscillations are small and increase rapidly with increasing frequency until a maximum is reached at about 0.1 cps. The theory predicts an increase in amplitude by a factor of 4, while the data show an increase of about 2.5. The shape of both the amplitude and phase agree well over the whole frequency range.

The change in the pressure variations for the two operating points may be understood more clearly by comparing the relative amplitudes of the frequency responses, as shown in figure 9. The amplitude for case II is normalized relative to the steady-state variations obtained for case I.

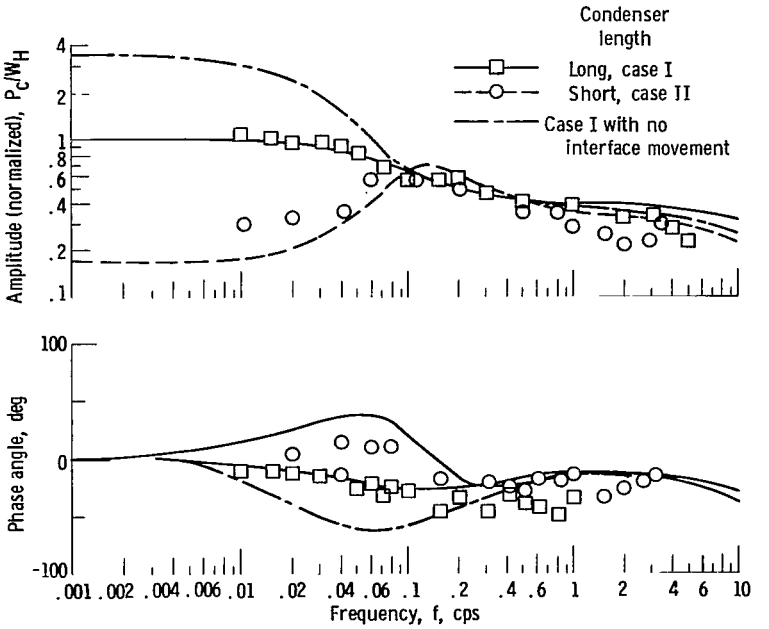

Figure 9. - Change in condensing pressure frequency response illustrating effect of interface movement.

The difference in amplitude may be attributed primarily to the change of the sensitivity of condensing pressure to interface movement. First the percent change in heat-transfer area per inch of condensing length is greater for the short condensing length of case II than for the long condensing length of case I. Also, for case II, the marked decrease in pressure drop for the shorter condensing length allows the condensing pressure to deviate less from the constant receiver pressure.

As a further ramification of the effect of interface movement on the pressure response, the hypothetical predicted pressure response with no interface movement is shown as the dotted line. This curve was obtained by substituting the appropriate parameter values of case I into equation (26). Note that it represents a specific instance of the general shape of the predicted frequency response of figure 5(a) (p. 17), which was discussed in the theory section.

With no interface movement, the pressure amplitudes as seen in the figure are three times higher at the lower frequencies than for case I. At the higher frequencies the differences between all three curves becomes much smaller, since the interface response declines above 0.1 cps, as will be seen next.

The frequency responses for the interface G_{1L} for both cases are shown in figure 10. The data points correspond to case I. The data for case II are not available due to lack of instrumentation at the short condensing length.

The predicted and measured amplitudes of the interface movements agree remarkably well. The phase does not agree, however, and the measured phase lag increases much more rapidly than the theory would predict. This discrepancy is most probably due

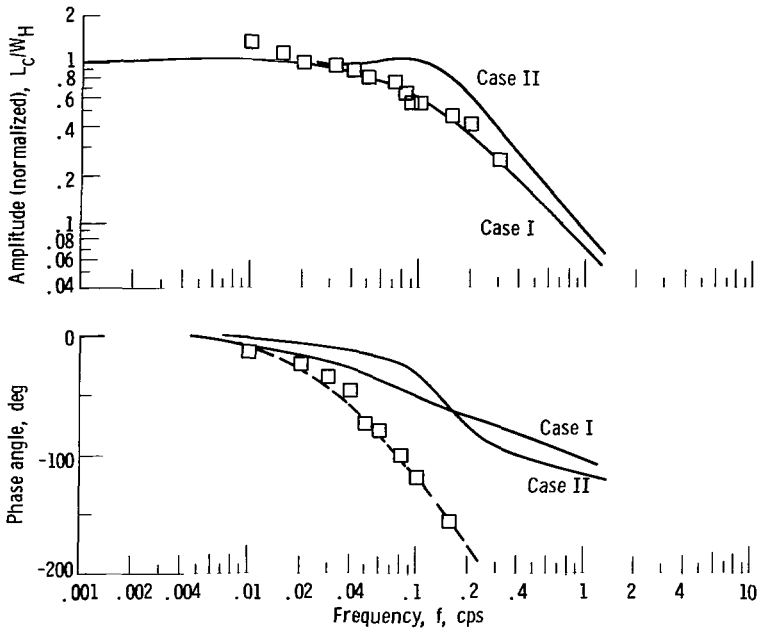

Figure 10. - Experimental and theoretical frequency response of interface movement to vapor flow for cases I and II.

to neglecting the transport delay of the condensate liquid droplets reaching the interface. The theory, in fact, assumes that as soon as the vapor condenses, the droplets arrive at the interface.

As a matter of interest, the addition of a pure delay, of the form $e^{-\tau s}$, to the frequency response introduces desired phase shift without changing the amplitude. A transport delay time of about 2 seconds (τ = 2) results in a phase shift characteristic as shown by the dotted line in figure 10, which agrees very closely with the measured values over all frequencies.

Unfortunately there does not seem to be a ready theory for predicting this particular delay, since the droplets form at various positions along the whole length of the tube wall and it is difficult if not impossible to predict their velocity distribution.

The dynamics of the interface can be characterized by a second-order lag and a first-order lead term. For a damping ratio of greater than 1 the lead term cancels with one of the lags so that a basic first-order lag response results as shown by case I. Where the system is slightly underdamped, a slight lead effect may result as shown by case II. The general characteristic remains that of a first-order lag. An additional lag comes into effect at the higher frequencies, but this is not felt until the amplitude has attenuated by a factor of 10. The major lag time constant is a function of the wall thermal capacitance and the liquid fill time of the condenser. At the higher frequency, the liquid column inertia and resistance may come into play. As discussed previously, the phase does not show the appropriate characteristic of a second-order system, but seems rather

to include a transport delay time which adds additional phase lag proportional to frequency.

It should be noted that on some of the subsequent data runs the interface movement showed considerable deviation from an idealized sinusoidal response, including some erratic behavior. This condition may be due to wetting of the tube by the mercury and/or to formation of large slugs of mercury in the condensing region which coalesce with the interface in random fashion. This type of deviation from the idealized mobile column of liquid cannot be predicted by the simplified model. Nevertheless, examination of the frequency responses for the previous conditions indicates that the break frequencies of both the interface and pressure responses can still be predicted by the theory with good accuracy.

Sensitivity of Predicted Frequency Response to Parameter Changes

Some of the constants used in the calculations of the frequency response are generally not accurately known and may change during the operation of the process. The problem, which is to estimate how these inaccuracies effect the success of predicting dynamic behavior, is studied by varying the more uncertain properties and calculating the resultant changes in the theoretical frequency responses.

Four parameters are investigated. Two of them are the partial derivatives of the vapor pressure drop functions q_v ($\partial q_v/\partial \ell_c$ and $\partial q_v/\partial w_H$). These are difficult to predict or measure accurately, and they may have a significant effect on the way the condenser responds. The third parameter is the partial derivative of the pressure drop in the liquid region ($\partial q_L/\partial w_L$), which enters into the determination of the liquid column movement. The fourth is the steady-state tube wall temperature T_w, which is used to calculate the coefficients of heat transfer and hence may introduce uncertainty in the thermal time constant of the wall.

Each of the previous four variables is varied one at a time about the reference value of case I. The amount of variation depends on the uncertainty of the particular property. For each variation the transfer function parameters are calculated and the resultant frequency response compared to that of case I. The results are summarized in table I. The first column identifies the variable and its units. The second column shows the high and low values of each of the variables. The third column indicates the calculated change in the amplitude and phase in frequency response of the condensing pressure. The amounts shown are the maximum percent change in the amplitude plot, and the maximum difference of phase in degrees. Where the amount of deviation is significant (greater than +25 percent), the actual frequency response plots are presented. Only two of the parameter changes have a significant effect on the pressure response amplitude. These

TABLE I. - COMPARISON OF CHANGES IN PREDICTED FREQUENCY RESPONSES DUE TO UNCERTAINTY OF VARIOUS TRANSFER FUNCTION PARAMETERS

Parameter variable	Variable values		Maximum changes in $G_{1p}(jf)$		Variation of pressure steady-state gain, K_{1p}	Maximum changes in $G_{1L}(jf)$		Variation of pressure steady-state gain, K_{1L}
			Amplitude, percent	Phase, deg		Amplitude, percent	Phase, deg	
$\frac{\partial q_v}{\partial \ell_c}$, $\frac{(lb/ft^2)}{ft}$	High	1 150	-25	10	17 percent	-10	---	-6.4 percent
	Reference	965	Significant sensitivity		1.35	Insignificant sensitivity		0.732
	Low	720	50	-10	-30 percent	10	---	10 percent
$\frac{\partial q_v}{\partial w_H}$, $\frac{(lb/ft^2)}{(lb/sec)}$	High	-70 000	25	-5	-15 percent	-25	-5	5.2 percent
	Reference	-46 500	Insignificant sensitivity		1.35	Insignificant sensitivity		0.732
	Low	-20 000	-16	5	18.5 percent	22	10	-6.5 percent
$\frac{\partial q_L}{\partial w_L}$, $\frac{(lb/ft^2)}{(lb/sec)}$	High	3 660	10	5	1 percent	-30	12	-1 percent
	Reference	2 740	Insignificant sensitivity		1.35	Significant sensitivity		0.732
	Low	1 830	-17	-5	-1 percent	50	-12	1 percent
T_w, ^oF	High	650	-50	16	No change	-20	5	No change
	Reference	630	Significant sensitivity		1.35	Insignificant sensitivity		0.732
	Low	610	50	-10	No change	10	-5	No change

are the first parameter $\partial q_v/\partial L_c$, which is defined as the partial of vapor pressure drop to changes in condensing length, and the fourth parameter T_w, which is the wall temperature. The resultant variations in frequency responses are given in figures 11(a) and (b), respectively.

The lower value of $\partial q_v/\partial L_c$ has the effect of increasing the predicted frequency range for which a steady amplitude is maintained. Increasing $\partial q_v/\partial L_c$ brings about a faster decline of amplitude with frequency.

Changes in wall temperature show a slightly different effect. Apparently only the time constant of the wall τ_w is changed significantly by this variation. Since the factor $1 + \tau_w s$ enters directly into the numerator of the pressure response transfer function, this element acts directly as a lead. As τ_w increases, the lead effect is felt earlier

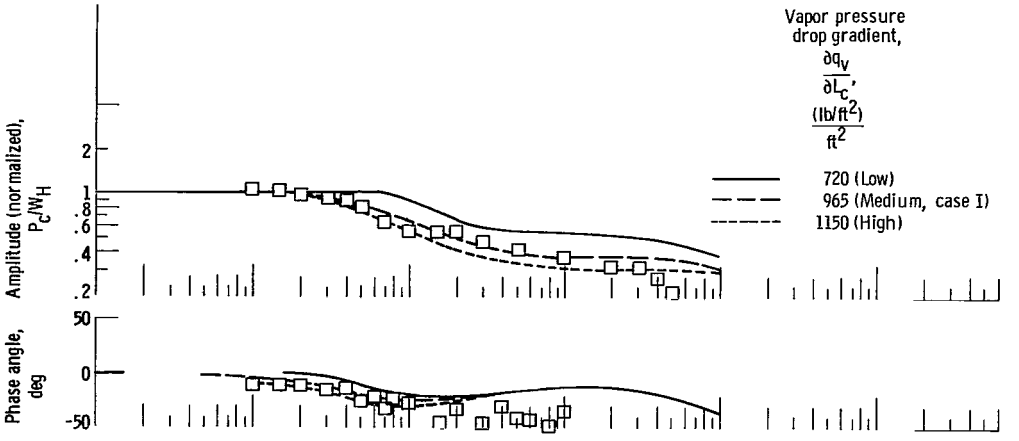

(a) Due to uncertainty in vapor pressure drop gradient.

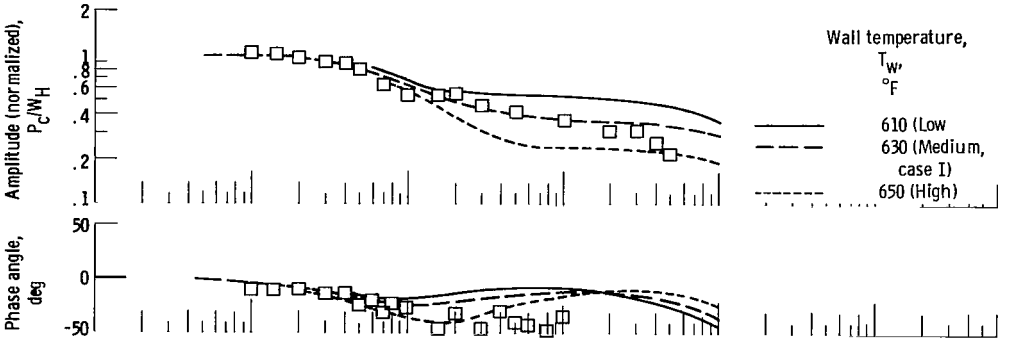

(b) Due to uncertainty in wall temperature.

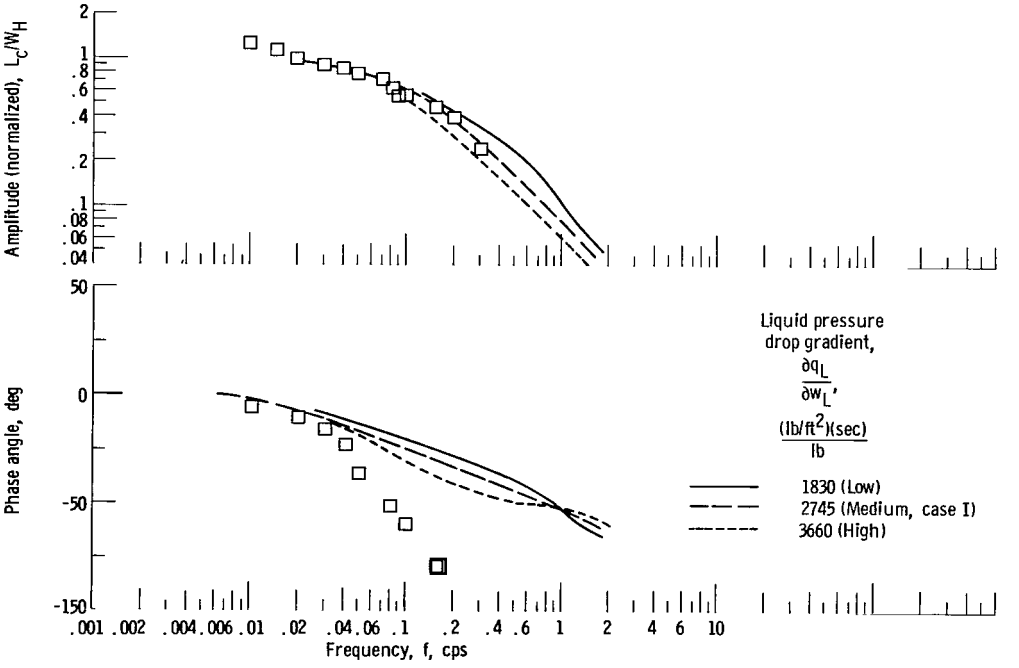

(c) Due to uncertainty of liquid pressure drop gradient.

Figure 11. - Variations of predicted frequency response of condenser variables to vapor flow.

and the pressure amplitude remains higher. Decreasing τ_w (increasing T_w) allows a greater decline of amplitude before the lead effect is felt. This shift in corner frequency of the lead element is also substantiated by the shift in the phase lag.

The fourth column of table I gives the predicted dimensionless amplitude gain of the pressure response under steady-state conditions, as defined by K_{1p} of equation (35a). Only the first and second variables show a significant effect on this amplitude.

The next column shows the change in amplitude and phase of the interface response, again as referred to case I. Although there is some variation in frequency response in all cases, only variations in the liquid pressure drop q_L seem to be of significance. The result is shown in figure 11(c). The major deviations come at the higher frequencies. This agrees with expectation since the time constants of the liquid column which are directly proportional to $\partial q_L/\partial w_L$ are significant only at high frequencies. The last column, which tabulates the gains of the interface movements as defined by K_{1L} of equation (37a), shows that only the two vapor pressure drop partials are of importance in predicting the steady-state amplitudes.

The general conclusions that can be drawn from the study of the sensitivity of the predicted frequency responses to uncertainty in the process parameters are the following:

(1) The change of vapor pressure drop with condensing length and, in general, the heat-transfer coefficients of the tube have a significant effect on the predicted dynamic response of the condensing pressure. Thus it is important to determine these particular variables accurately.

(2) The prediction of the dynamics of the interface movement is not very sensitive to the parameter variations. Only the liquid pressure drop characteristic as defined by $\partial q_L/\partial w_L$ has a significant influence on the normalized frequency response and this only at the higher frequencies.

Theory Simplification

Although it has been shown that the dynamic behavior of the condensing pressure and interface can be successfully predicted, the required calculations are quite long and difficult. Furthermore, the complexity of the parameters of the two transfer functions as given in table II obscures the influence of the basic time constants discussed in the earlier sections of the theory. That some of the terms in the polynomials and constants are insignificant is substantiated by their relatively small numerical value and by the small effect that variations of these parameters have on the frequency response as seen in the previous section. Consequently, simplification of the theory is desirable and is possible, as will be shown in this section.

The method of simplification is to start with the examination of the numerical values

of the coefficients of G_{1p} and G_{1L} as given in table II. For both cases it is evident that the coefficients N_2, D, and C of G_{1p} and M_{2L} and M_{3L} of G_{1L} are more than an order of magnitude smaller than the other coefficients. Whether all these are small for every condenser is questionable; consequently, for different configurations and condensing fluids a quick check of the relative size of the coefficients should be made. For the condensing tube studied, however, the simplifications are apparently valid for the various operating points.

In addition to neglecting some of the coefficients, the form of the remaining constants A, B, N_1, and M_{1L} can be further simplified by dropping those terms in their calculations that are small. Their relative size is determined by examining the numerical values as given in table IV. After eliminating the terms containing θ, τ_p, and τ_{1p}, the coefficients of the transfer function polynomials can be written as

$$A' = \frac{\frac{\theta_r}{K_v} + \tau_{1w} + \beta_g \tau_w}{1 + \beta_g} \tag{40}$$

$$B' = \frac{\tau_{1w}\theta_r}{K_v(1 + \beta_g)} \tag{41}$$

$$N_1' = \frac{\theta_r}{K_v + K_w + 1} \tag{42}$$

$$M_{1L}' = \frac{\tau_w - \beta_p \tau_{1w}}{1 - \beta_p} \tag{43}$$

The resultant simplified form of the transfer functions G_{1p} and G_{1L} are

$$G_{1p}' = \frac{(1 + \tau_w s)(1 + N_1' s)}{1 + A's + B's^2} \tag{44}$$

$$G_{1L}' = \frac{1 + M_{1L}' s}{1 + A's + B's^2} \tag{45}$$

The validity of these simplifications must be checked by comparing the resultant frequency response with the unsimplified cases. The new constants are calculated by using the applicable numerical values used for cases I and II in table IV. The expressions for the frequency responses for the simplified cases I and II are given in equations (46) to (49):

Case I:

$$G'_{1p}(w) = \frac{\left(1 + \frac{jf}{0.187}\right)\left(1 + \frac{jf}{0.106}\right)}{\left(1 + \frac{jf}{0.064}\right)\left(1 + \frac{jf}{0.121}\right)} \tag{46}$$

$$G'_{1L}(w) = \frac{1 + \frac{jf}{0.0755}}{\left(1 + \frac{jf}{0.064}\right)\left(1 + \frac{jf}{0.121}\right)} \tag{47}$$

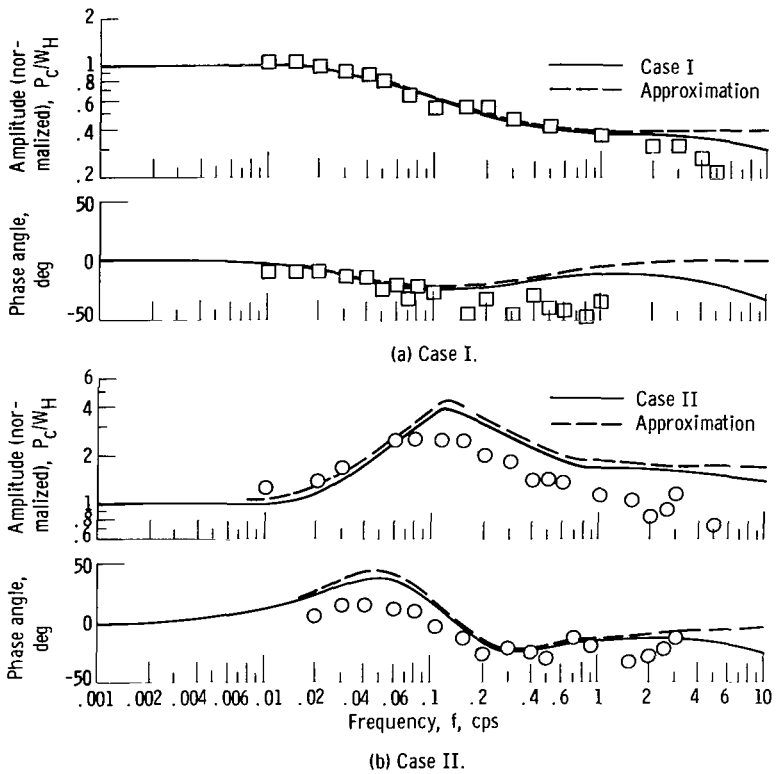

Figure 12. - Comparison of approximation to original theory for condensing pressure response.

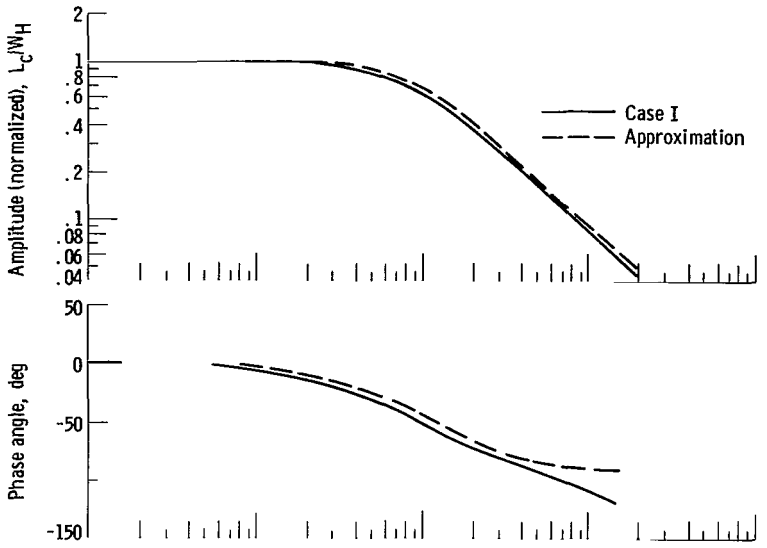

(a) Case I.

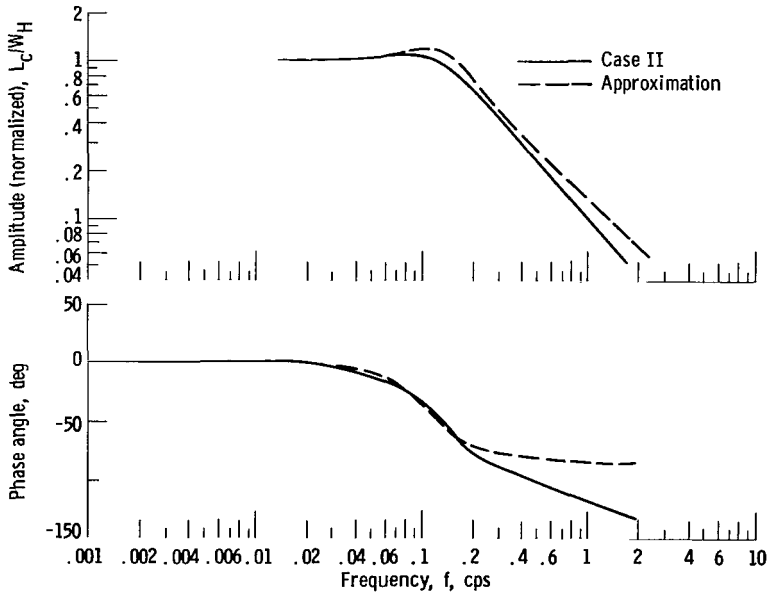

(b) Case II.

Figure 13. - Comparison of approximation to original theory for interface response.

Case II:

$$G'_{1p}(w) = \frac{\left(1 + \frac{jf}{0.338}\right)\left(1 + \frac{jf}{0.0241}\right)}{1 + jf\frac{2(0.63)}{0.123} + \left(\frac{jf}{0.123}\right)^2} \tag{48}$$

$$G'_{1L}(w) = \frac{1 + \frac{jf}{0.109}}{1 + jf\frac{2(0.63)}{0.123} + \left(\frac{jf}{0.123}\right)^2} \tag{49}$$

These equations are plotted in figures 12 and 13. The solid lines show the previous prediction of the unsimplified theory. As can be seen from the figures, good agreement is obtained with the previously predicted condensing pressure responses for frequencies up to approximately 3 cps. The interface amplitude agrees well up to 1 or 2 cps, but the phase begins to show a marked difference at even lower frequencies for both cases. These differences are as expected since the neglected time constants would begin to show their effect at these higher frequencies.

Thus, it can be concluded that a good estimate of the frequency response behavior of the condenser up to approximately 1 cps can be obtained by the simplified transfer functions. The condensing pressure response to flow rate variations is given by equation (44). The corresponding interface movement is given by equation (45). The coefficients of the new transfer functions, as defined by equations (40) to (43), are much reduced in complexity. Their simplified form shows that basically only the three time constants τ_w, τ_{1w}, and θ_r, besides the various dimensionless gains, are important in determining the dynamic characteristics over the specified frequency range. The meaning of these parameters was discussed in the earlier sections where the interface movement and pressure response were treated independently.

The only limitations of using the simplified model are that (1) the frequency response is not as accurate at the higher frequencies where the neglected vapor volume capacitance and the liquid column time constant become dynamically significant, and (2) the neglected coefficients and parameters must be small.

CONCLUDING REMARKS

The linearized analysis of the condenser tube results in a set of transfer functions relating the dynamic behavior of condensing pressure and interface movement to various

input variables. The condensing pressure to vapor flow rate transfer function for a fixed interface is a lag-lead type for moderate frequencies. The time constants for this transfer function are related to the heat-transfer coefficients and the tube wall heat capacity. At high frequencies, an additional lag arising from the vapor volume capacitance comes into effect. The interface movement depends on the type of end conditions used for the condenser. For the constant pressure receiver, the interface responds to condensing pressure as a second-order system where the damping and natural frequency depends on the liquid column inductance, the pressure drop characteristic of both the vapor and liquid, and the liquid fill time of the condenser.

The condensing pressure transfer function, combined with the interface transfer function of a constant pressure receiver, was used to predict the behavior of a mercury condensing tube. The predicted condensing pressure frequency response to vapor flow variations agrees with the experimental values over a frequency range between 0 and 5 cps. The amplitude of the corresponding interface movement is also accurately predicted. The measured values of the phase of the interface, however, show a much greater lag than predicted. This is attributed to the delay of the liquid droplets reaching the interface which has been neglected in the theory.

The condensing pressure frequency response is sensitive to changes in the operating point especially when these changes involve the condensing length, heat-transfer coefficients, and some of the pressure drop characteristics. The responses are not so sensitive to many other system parameters, so that good prediction may be obtained without accurate knowledge of all the process properties.

Considerable simplification in the form and length of the polynomials of the two transfer functions relating condensing pressure and interface position to flow rate variations is made possible due to the insignificant magnitudes of some of the coefficients. The simplified model agrees very closely with the more complex theory except at the high frequencies above 1 cps where the inaccuracies would be expected.

Since the theory is derived for the general case of a crossflow cooled condenser, it may be concluded that the model will predict dynamic response of condensing pressure and interface movement in other condensers of this type. Where such condensers have entrance and exit conditions other than treated herein (choked inlet and a constant pressure received at outlet), the derivation still may be applied by addition of the proper pressure-to-flow impedance functions to the basic condenser model as given by equation (12). Several aspects of condenser dynamics, however, still need to be analyzed. Among these are the dynamic interaction between tubes in condensers of multitube construction

and the effects of coolant dynamics, particularly in liquid-cooled counterflow or parallel-flow condensers.

Lewis Research Center,
National Aeronautics and Space Administration,
Cleveland, Ohio, Februaty 14, 1966.

APPENDIX A

SYMBOLS

A, B, C, D	coefficients of denominator of transfer function, see table II
A_c	cross-sectional area of tube, $\pi D_1^2/4$
A', B'	simplified coefficients of transfer function, see equations (40) and (41)
a, b	coefficients of interface transfer function, see page 15
a_L, b_L	coefficients of transfer function, see table IV
a_s, b_s	coefficients of pressure transfer function, see page 10
C_n	dimensionless coolant temperature variation, $\Delta T_n/T_a$
c_w	specific heat of tube wall
D_1, D_2	inside and outside diameter of tube, respectively
f	frequency of sinusoidal disturbance, cps
f_n	natural frequency of second-order system, cps
G_i	transfer function of interface movement, see equation (25)
G_s	basic condensing pressure transfer function, see equation (12)
G_t	common term in condenser transfer functions, see equation (35g)
G_{1L}, G_{2L}, G_{3L}	interface transfer functions, see equations (37d), (37e), and (37f)
G'_{1L}	simplified G_{1L}, see equation (45)
G_{1p}, G_{2p}, G_{3p}	condensing pressure transfer functions, see equations (35d), (35e), and (35f)
G'_{1p}	simplified G_{1p}, see equation (44)
H_L	latent heat of vaporization
h_{cw}	coefficient of heat transfer between condensate and wall
h_{nw}	coefficient of heat transfer between coolant and wall
J	mechanical equivalent of heat
j	complex operator, $\sqrt{-1}$
K_p	$(\bar{p}_c/\bar{w}_H)/(\partial q_L/\partial w_L)$
K_t	$(Z_L \bar{p}_c/T_a)(dT_c/dp_c)$

K_v	$\bar{\ell}_c(\partial q_v/\partial \ell_c)/w_H(\partial q_L/\partial w_L)$
K_w	$(\partial q_v/\partial w_H)/(\partial q_L/\partial w_L)$
K_{1L}, K_{2L}, K_{3L}	dimensionless steady-state gains of interface transfer functions, see equations (37a), (37b), and (37c)
K_{1p}, K_{2p}, K_{3p}	dimensionless steady-state gains of condensing pressure transfer functions, see equations (35a), (35b), and (35c)
K_{1w}	$h_{cw}D_1/(h_{cw}D_1 + h_{nw}D_2)$
K_{2w}	$1 - K_{1w}$
k	proportionality constant for condensate liquid pressure drop, see equation (B4)
L_c	percent variation of condensing length, $\Delta\ell_c/\bar{\ell}_c$
ℓ_c	condensing length
ℓ_L	liquid column length
M_L	mass of mercury liquid column in condenser
M_{1L}, M_{2L}, M_{3L}	coefficients of transfer function for interface movement, see equation (37d)
M'_{1L}	simplified M_{1L}, see equation (43)
m	slope of condensing temperature profile
N_1, N_2	coefficients of pressure response transfer function, see equation (35d)
N'_1	simplified N_1, see equation (42)
P_c	percent condensing pressure variation at tube inlet, $\Delta p_c/\bar{p}_c$
P_r	percent receiver pressure variation, $\Delta p_r/\bar{p}_c$
p_c	condensing pressure
p_f	interface pressure
p_r	receiver pressure
q_L	pressure drop in liquid region
q_v	pressure drop in condensing region
R	gas constant
s	Laplace operator, sec^{-1}
T_a	average temperature difference between condensate and coolant, $\bar{T}_c Z_L - \bar{T}_N$

T_c	condensing temperature
$T_c(\bar{\ell}_c)$	condensing temperature at interface
T_n	coolant temperature
T_s	temperature drop in condensing region
T_w	wall temperature
$T_w(\bar{\ell}_c)$	wall temperature at interface
t	time, sec
V_c	volume of condensing region, $A_c\bar{\ell}_c$
V_v	volume of gas phase
v_L	velocity of liquid column
W_c	percent condensate flow variation, $\Delta w_c/\bar{w}_H$
W_H	percent flow variation, $\Delta w_H/\bar{w}_H$
W_L	percent liquid flow variation, $\Delta w_L/\bar{w}_L$
w_c	condensate flow rate
w_H	fluid flow rate into condensing region
w_L	liquid outflow rate from condenser
X_q	quality at inlet of tube
x	distance from inlet of tube
Z_L	temperature averaging coefficient, $1 - (m\bar{\ell}_c/2)$
β_g	dimensionless coefficient, K_p/K_vK_t
β_p	dimensionless coefficient, $K_t(1 + K_w)/K_p$
β_v	dimensionless coefficient, $(1 + K_w)/K_v$
β_x	vapor density coefficient, $\bar{p}_c/\bar{\rho}_vH_LJ$
θ	vapor fill time of condenser, $V_v\bar{\rho}_v/\bar{w}_HX_q$
θ_r	liquid fill time of condenser, $V_v(\rho_L - \rho_v)/\bar{w}_H$
ρ_L	density of liquid condensate
ρ_v	density of vapor
ρ_w	density of tube wall
τ_p	time constant of liquid column movement, $\ell_L/A_c(\partial q_L/\partial w_L)$

τ_w	time constant of heat flow into wall, $\tau_{1w}h_{nw}D_2/(h_{nw}D_2 + h_{cw}D_1)$
τ_1, τ_2	factors of quadratic term in G_s, see equations (27) and (28)
τ_{1a}, τ_{2a}	simplified τ_1 and τ_2, see equations (29) and (30)
τ_{1p}	$\tau_p/(1 + K_w)$
τ_{1w}	time constant of heat flow into wall, $\rho_w c_w \left(D_2^2 - D_1^2\right)/4h_{nw}D_2$
σ	damping ratio of second-order system
Δ	increment of variation of
–	value of variable at steady state

APPENDIX B

CALCULATION OF PARAMETERS FOR CONDENSER TRANSFER FUNCTIONS

The two transfer functions of interest relating the condensing pressure and vapor-liquid interface movement to vapor flow rate variations are

$$\frac{P_c}{W_H} = \frac{K_{1p}(1 + \tau_w s)\left(N_2 s^2 + N_1 s + 1\right)}{Ds^4 + Cs^3 + Bs^2 + As + 1} \tag{B1}$$

$$\frac{L_c}{W_H} = \frac{K_{1L}\left(1 + M_{1L} s - M_{2L} s^2 - M_{3L} s^3\right)}{Ds^4 + Cs^3 + Bs^2 + As + 1} \tag{B2}$$

The transfer function parameters and their definitions are tabulated for the various cases investigated as given in table II. These constants were calculated by using the values of the process variables and dimensions at the operating point. An example of these calculations is presented herein.

The basic system constants needed for the calculation of the transfer function parameters are given in table III. The first group is easily obtained from the dimensions of the tube, the gage readings, or from the material properties. The second and third groups of constants are calculated from the steady-state data. The calculations for case I are presented as an example.

The slope m is calculated directly from the condensing temperature profile as shown in figure 14:

$$m = \frac{T_c(0) - T_c(\bar{\ell}_c)}{T_c(0)\,\bar{\ell}_c} = \frac{680 - 625}{680 \times 6.23} = 0.013 \text{ ft}^{-1}$$

The parameter Z_L, as defined in equation (12b), gives

$$Z_L = 1 - \frac{m\bar{\ell}_c}{2} = 1 - \frac{0.013 \times 6.23}{2} = 0.96$$

The average temperature difference is then

$$T_a = T_c(0)Z_L - T_n(0) = 680(0.96) - 170 = 483^{\circ} \text{ R}$$

TABLE II. - DIMENSIONLESS TRANSFER FUNCTION GAINS AND TIME CONSTANT PARAMETERS

Transfer function parameter	Case I	Case II
$K_{1p} = \frac{1 + \beta_v}{(1 + \beta_g)K_t}$	1.35	0.264
$K_{1L} = \frac{(1 - \beta_p)K_p}{K_t K_v (1 + \beta_g)}$	0.732	0.948
$\tau_w = \frac{\rho_w c_w (D_2^2 - D_1^2)}{4(h_{cw} D_1 + h_{nw} D_2)}$, sec	0.851	0.471
$N_1 = \frac{b + \beta_v(\tau_{1p} + \theta)}{1 + \beta_v}$, sec	1.485	5.71
$N_2 = \frac{a + \beta_v \theta \tau_{1p}}{1 + \beta_v}$, sec^2	0.075	0.46
$A = \frac{b + b_s + b_L \beta_g}{1 + \beta_g}$, sec	3.86	1.66
$B = \frac{a_s + a + b_s b + \beta_g a_L}{1 + \beta_g}$, sec^2	3.40	1.73
$C = \frac{a_s b + b_s a}{1 + \beta_g}$, sec^3	0.208	0.149
$D = \frac{a_s a}{1 + \beta_g}$, sec^4	0.00202	0.00104
$M_{1L} = \frac{\tau_w - \beta_p(b_s + \tau_{1p})}{1 - \beta_p}$, sec	1.66	1.11
$M_{2L} = \frac{(a_s + b_s \tau_{1p})\beta_p}{1 - \beta_p}$, sec^2	-0.0081	-0.00235
$M_{3L} = \frac{a_s \tau_{1p} \beta_p}{1 - \beta_p}$, sec^3	0.000035	0.00002

TABLE III. - BASIC SYSTEM CONSTANTS FOR TWO OPERATING POINTS

Variable	Case I	Case II
Directly read variables and constants		
D_1, ft	0.0255	0.00255
D_2, ft	0.0306	0.0306
A_c, ft^2	0.000508	0.000508
c_w, Btu/(lb)(^oF)	0.11	0.11
ρ_w, lb/ft^3	490.0	490.0
$\overline{\rho}_v$, lb/ft^3	0.225	0.33
ρ_L, lb/ft^3	792.0	790.0
w_H, lb/sec	0.0315	0.035
$\overline{\ell}_c$, ft	6.23	4.16
ℓ_L, ft	2.27	4.34
p_c, lb/ft^2	2232.0	3040.0
$T_c(0)$, ^oF	680.0	710.0
X_q, dimensionless	1.0	1.0
H_L, Btu/lb	126.1	126.0
$T_n(0)$, ^oR	630.0	630.0
$T_w - T_n$, ^oR	410.0	495.0
$T_c - T_w$, ^oR	65.0	45.0
Calculated constants		
m, ft^{-1}	0.013	0.002
Z_L, dimensionless	0.96	0.996
T_a, ^oF	482.0	537.0
h_{nw}, $\frac{Btu}{(ft^2)(^oR)(sec)}$	0.0153	0.0224
h_{cw}, $\frac{Btu}{(ft^2)(^oR)(sec)}$	0.159	0.294
$V_c = A_c \overline{\ell}_c$, ft^3	0.00317	0.00213
Parameter variables		
$\frac{\partial q_L}{\partial w_L}$, $\frac{(lb/ft^2)(sec)}{lb}$	2750	3300
$\frac{\partial q_v}{\partial \ell_c}$, $\frac{(lb/ft^2)}{ft}$	965	750
$\frac{\partial q_v}{\partial w_H}$, $\frac{(lb/ft^2)(sec)}{lb}$	-46 500	-65 000
$\frac{dT_c}{dp_c}$, $\frac{^oR}{(lb/ft^2)}$	0.0445	0.035
T_s, ^oR	55.0	6.0
$T_w(0)$, ^oR	1090	1125
$T_w(0) - (T_s/2)$, ^oR	602	662

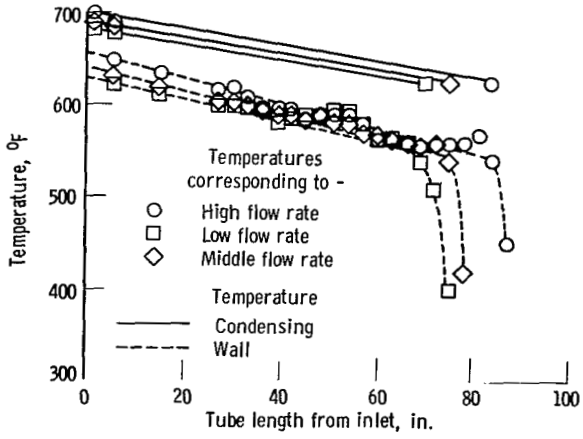

Figure 14. - Typical temperature profile variation due to changes in mercury flow rate and condensing length.

The heat-transfer coefficients h_{nw} and h_{cw} are obtained by employing the measured average temperature difference between the wall and coolant and wall and condensing vapor under steady-state conditions when the heat flux rate is known:

$$h_{nw} = \frac{H_L{}^{w}H^{X}q}{\pi D_1 \bar{\ell}_c \left(\overline{T}_w - \overline{T}_n\right)} = \frac{(126.1)(0.0315)(1.0)}{(3.14)(0.0306)(6.23)(602 - 170)} = \frac{0.0153 \text{ Btu}}{(^{o}R)(\text{sec})(\text{ft}^2)}$$

where

$$\overline{T}_w = T_w(0) - \frac{T_c(0) - T_c(\bar{\ell}_c)}{2} = 630 - \frac{55}{2} = 602$$

and similarly,

$$h_{cw} \cong \frac{H_L{}^{w}H^{X}q}{\pi D_1 \bar{\ell}_c \left[T_c(0) - T_w(0)\right]} = 0.159$$

The condensing volume V_c is the product of the cross-sectional area and the condensing length:

$$V_c = A_c \bar{\ell}_c = 3.17 \times 10^{-3} \text{ ft}^3$$

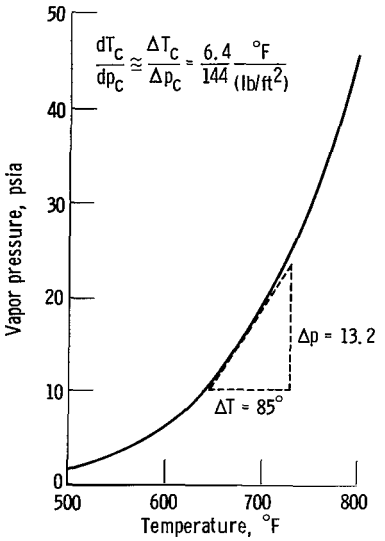

Figure 15. - Vapor pressure curve for mercury illustrating calculation of the local slope of the saturation curve (dT_c/dp_c).

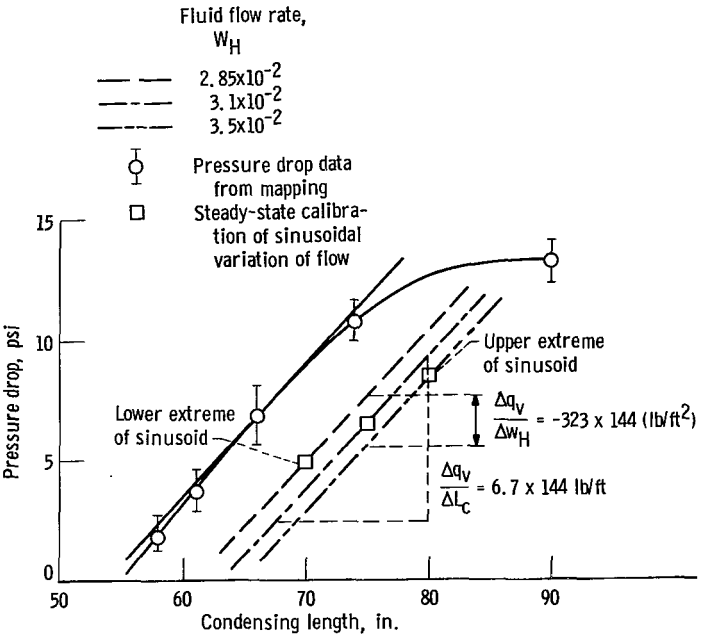

Figure 16. - Example of graphical estimation of pressure drop gradients $\partial q_v/\partial w_H$ and $\partial q_v/\partial L_c$ for variations about steady-state operating point.

Calculation of Partial Derivatives

The derivative dT_c/dp_c is by definition the slope of the mercury saturation curve. It can be calculated by using the Clausius-Clapyron relation as given by equation (7) or by graphical means. The later method is employed for case I as shown in figure 15:

$$\frac{dT_c}{dp_c} = 0.044 \frac{°F}{lb/ft^2}$$

A fairly simple method was devised for evaluating the two partial derivatives $\partial q_v/\partial \ell_c$ and $\partial q_v/\partial w_H$. The method depends on obtaining a single experimental map of q_v against L_c for constant vapor flow in the vicinity of the operating point in addition to the three points of pressure drops against condensing length at the midpoint and the two extremes of the flow perturbations. The partials can then be evaluated as shown in figure 16. The partial $\partial q_v/\partial L_c$ is obtained from the straight line approximation to the experimental map as indicated by circular data points. When lines of the same slope are drawn through the two points (indicated by a square) obtained from the flow variations and the vertical distance between them is measured, the other partial $\partial q_v/\partial w_H$ is determined.

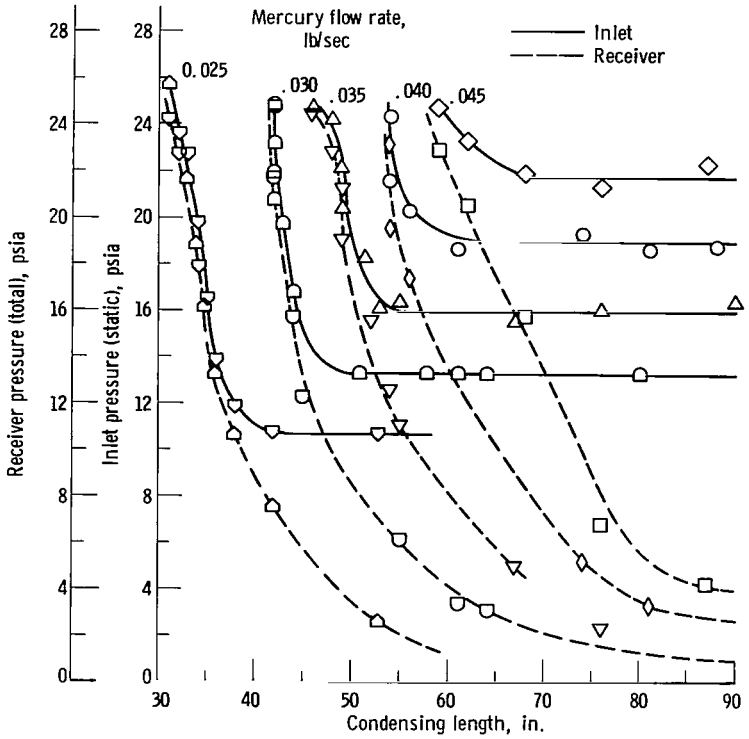

Figure 17. - Steady-state map at 5.0 psid coolant.

The negative value of $\partial q_v/\partial w_H$ that results for both cases is not easily explained by steady-state analytic calculations. The result is substantiated, however, by the experimentally determined steady-state mapping of the condenser operation. A typical plot of condenser inlet pressure and receiver pressure against condensing length for a gas coolant rate, such as used for case II, is shown in figure 17. The solid lines are the condensing inlet pressures with constant mercury vapor flow as the parameter. The dotted lines are the receiver pressures corresponding to the inlet pressures. The pressure difference between each pair of lines represents the pressure drop of the condenser which, except for the small liquid pressure drop, is equal to q_v. The variation of q_v with flow rate can be obtained by measuring the pressure drop for each flow rate at a constant condensing length.

The last partial derivative of liquid pressure drop to flow variations $\partial q_L/\partial w_L$ is not easily evaluated, since the liquid pressure drop is small and the pressure transducers in the liquid mercury exhibit much noise. Estimation from the recorded traces indicate approximately 0.2-psi pressure drop through the wide open exit valve at the midrange flow. Other pressure drop measurements indicate an additional liquid friction drop in the tube from 0.1 to 0.4 psi depending on the liquid length. When an orifice type restriction is assumed, the liquid pressure drop would obey a square law relation as shown in equation (B3):

"The aeronautical and space activities of the United States shall be conducted so as to contribute . . . to the expansion of human knowledge of phenomena in the atmosphere and space. The Administration shall provide for the widest practicable and appropriate dissemination of information concerning its activities and the results thereof."

—NATIONAL AERONAUTICS AND SPACE ACT OF 1958

NASA SCIENTIFIC AND TECHNICAL PUBLICATIONS

TECHNICAL REPORTS: Scientific and technical information considered important, complete, and a lasting contribution to existing knowledge.

TECHNICAL NOTES: Information less broad in scope but nevertheless of importance as a contribution to existing knowledge.

TECHNICAL MEMORANDUMS: Information receiving limited distribution because of preliminary data, security classification, or other reasons.

CONTRACTOR REPORTS: Technical information generated in connection with a NASA contract or grant and released under NASA auspices.

TECHNICAL TRANSLATIONS: Information published in a foreign language considered to merit NASA distribution in English.

TECHNICAL REPRINTS: Information derived from NASA activities and initially published in the form of journal articles.

SPECIAL PUBLICATIONS: Information derived from or of value to NASA activities but not necessarily reporting the results of individual NASA-programmed scientific efforts. Publications include conference proceedings, monographs, data compilations, handbooks, sourcebooks, and special bibliographies.

Details on the availability of these publications may be obtained from:

SCIENTIFIC AND TECHNICAL INFORMATION DIVISION

NATIONAL AERONAUTICS AND SPACE ADMINISTRATION

Washington, D.C. 20546